Bull. Mater. Sci. (2022) 45:159
https://doi.org/10.1007/s12034-022-02734-0

Charge and rigidity effects on the encapsulation of quercetin by multilamellar vesicles

LUCIANA CUSTÓDIO[1,†], LEANDRO ANTUNES MENDES[1,†], DAYANE S ALVARES[2], JÉFERSON APARECIDO MORETO[1] and NATÁLIA BUENO LEITE SLADE[1,*]

[1]Department of Physics, Federal University of Triângulo Mineiro, Uberaba 38064-300, Brazil
[2]Department of Physics, São Paulo State University, São José do Rio Preto, SP 15054-000, Brazil
*Author for correspondence (natalia.slade@uftm.edu.br)

[†]These authors have contributed equally to this study.

MS received 22 December 2021; accepted 18 April 2022

Abstract. Although quercetin has a wide range of applications due to its biological properties, its activity may be affected due to its low solubility and its potential for degradation in a physiological environment. The nanoparticulate and microparticulate systems appear as a powerful strategy to enhance its biological activity as well as to contribute to the viability of this compound for pharmacological purposes. Here, we present an innovative and applied research to study the effect of different lipid compositions on the encapsulation of quercetin by using multilamellar vesicles (MLVs). For this purpose, the effects of charge and rigidity in the formulation's average size, size distribution, charge properties, encapsulation and release efficiencies of this polyphenol were explored. Our results demonstrated that the rigidity imposed by cholesterol increased both the homogeneity of the size distribution and the encapsulation efficiency enabling a significant rate of quercetin release at the system with 1-palmitoyl-2-oleoyl-*sn*-glycero-3-phosphocholine/cholesterol (80:20). The charge modulated both the average size and size distribution as well as resulted in high encapsulation and release efficiencies in the formulation composed by (1-palmitoyl-2-oleoyl-*sn*-glycero-3-phosphocholine/1-palmitoyl-2-oleoyl-*sn*-glycero-3-phosphatidylglycerol (80:20). To the best of our knowledge, this is the first study concerning charge and rigidity effects on the encapsulation of quercetin in MLVs. Furthermore, the findings presented in this work is a starting point on the use of lipid composition as a modulating agent of important parameters in the development of nano and micro systems for controlled release.

Keywords. Nano/microparticulate systems; multilamellar vesicles; release assays; quercetin; lipid composition.

1. Introduction

Quercetin is a polyphenolic molecule presenting a wide range of biological activities, such as antioxidants, anticancer, antibacterial and antiviral [1–3]. However, its use for pharmacological purposes presents difficulties related to its low bioavailability and solubility in aqueous environment, high propensity to degradation against light, heat and oxygen, as well as its reduced biological activity towards the gastrointestinal tract [4]. Seeking to overcome these issues by improving the performance of quercetin as a medicine, many efforts have been made using its encapsulation in nano and microstructures as a delivery route to the systems of interest. This strategy has already been performed and involves the most diverse materials from synthetic and natural polymers to those based on lipid molecules [4–8], increasing the flavonoid's bioavailability as well as enhancing its action.

Liposomes are lipid-based structures that are especially attractive to nanocarriers because they are non-toxic and show significant similarity to several cellular structures that favour their internalization into cells and drug transport across membranes [9]. Drug-loaded liposomes are the most successful nanomedicine to date, with multiple systems approved by the United States Food and Drug Administration (FDA) for a multitude of diseases [10]. These structures are spherical and composed of one or more lamellae formed by highly ordered lipid bilayers. The encapsulation in multilamellar vesicles (MLVs) represents a low-cost alternative that is suitable for encapsulating hydrophobic bioactive molecules. That is successfully used in several areas from vaccine manufacturing to delivery of bioactive components (vitamin C, E, fish oil), targeting and enhancing antibacterial agents, and cosmetic applications [11–14]. However, there are

Supplementary Information: The online version contains supplementary material at https://doi.org/10.1007/s12034-022-02734-0.

Published online: 08 August 2022

difficulties in dealing with this system, which are related to controlling the encapsulation rate, membrane stability and degradation [11,15].

Given the versatility of preparing these structures, it is interesting to consider the variety of lipids and sterols found in nature. Lipids are amphipathic molecules exhibiting a polar head and a hydrophobic tail. They present variations in the net electrical charge of the heads, the amount of unsaturation in the tails, and the molecular geometry (given the volumetric proportions between head and tails) [16,17]. These aspects directly impact the biophysical properties of the lipid bilayers composed by them, enabling the production of liposomes with distinct charge, fluidity and morphological properties. There are still sterols, hydrophobic molecules, which can promote the stiffening of lipid bilayers by decreasing molecular free-volumes and increasing the order of the lipid acyl chains [18–21]. Depending on the cholesterol fraction in each composition, it is possible to change the membrane phase and influence the ordering of lipids [22,23].

Although many efforts have already been made in the study of the effect of lipid compositions to understand the interaction of bioactive and biological membranes, there is a lack of knowledge regarding the effect of different mixtures in the formulation of systems for controlled release. In this sense, here we present innovative research to study the influence of lipid composition in the encapsulation of quercetin by MLVs. By considering the effects of charge and rigidity in the formulation's average size, size distribution, charge properties besides the encapsulation and release efficiencies of this polyphenol. To the best of our knowledge, this is the first study concerning charge and rigidity effects on the encapsulation of quercetin in MLVs, with great potential to be used for pharmacological purposes. In addition, the results presented in this survey are a starting point on the use of lipid composition as a modulating agent of important parameters in the development of nano and microparticulate systems.

2. Experimental

2.1 *Chemicals*

Phospholipids and cholesterol (Chol), 1-palmitoyl-2-oleoyl-*sn*-glycero-3-phosphocholine (POPC) and 1-palmitoyl-2-oleoyl-*sn*-glycero-3-phosphatidylglycerol (POPG), were obtained from Avanti Polar Lipids®. Quercetin, HEPES and NaF were supplied by Sigma-Aldrich Co. (St. Louis, MO). Other chemicals were of high-quality analytical or spectroscopic grade.

2.2 *Quercetin solution and buffer preparation*

For partition coefficient determination, quercetin solutions were prepared by diluting 2 mg in 1.5 ml of 0.6% (v/v) dimethyl sulphoxide (DMSO) due to its low solubility in pure water by avoiding DMSO effects on the vesicles. The experiments were performed at pH 7.4 with a buffer solution composed of 20 mmol l^{-1} HEPES and 150 mmol l^{-1} NaF.

2.3 *Preparation of large unilamellar vesicles for partition coefficient assays*

Lipid stock solutions were mixed in chloroform to give the following compositions: POPC/POPG (80:20) and POPC/Chol/POPG (60:20:20), at the approximate concentration of 3 mmol l^{-1}. Lipid mixtures were submitted to evaporation of the solvent under N_2 flow followed by drying under vacuum over 3 h. The films were hydrated by the addition of a 20 mmol l^{-1} HEPES buffer containing 150 mmol l^{-1} NaF, pH 7.4. This suspension was homogenized by vortexing for 2.5 min. To obtain the large unilamellar vesicles (LUVs), after homogenization, the suspension was subjected to extrusion through polycarbonate membranes (6 and 11 times in 400 and 100 nm pore-size membranes, respectively) in an Avanti mini extruder. LUVs were kept under refrigeration, protected from light, and used within 24 h of preparation. LUVs were obtained with an average diameter of 110 to 140 nm and polydispersity index ranging from 0.10 to 0.15 as confirmed by dynamic light scattering measurements by using a ZetaSizer NanoZS (Malvern Instruments, Worcestershire, UK).

2.4 *Spectrophotometric titration*

Spectrophotometric measurements were performed in the presence of buffers or LUVs of different compositions to obtain the calibration curve of quercetin and the adsorption isotherms for partition coefficient, K_P, determination. At each aliquot added, either of the quercetin stock solution (0 to 50 μmol l^{-1}), in the experiment to determine calibration curve, or of the vesicle suspension (0 to 700 μmol l^{-1}) to determine K_P, an absorption spectrum was recorded from 300 to 500 nm with a UV–Vis's spectrophotometer Shimadzu UV 2600 model (Shimadzu Corp, Japan). Spectra were corrected for dilution effect with the subtraction of respective baselines. The second derivative was obtained to determine the wavelength of maximum absorbance [24]. K_P values were determined by fitting plots with the equation (1):

$$\frac{Abs(L)}{Abs_0} = 1 + \left(\frac{Abs_{\max}}{Abs_0} - 1\right) \times \frac{K_p \gamma_L [L]}{1 + K_p \gamma_L [L]} \quad (1)$$

where Abs(L), Abs_0 and Abs_{max} are the absorbance in the presence and absence of LUVs, and the maximum absorbance obtained; [L] is the phospholipid concentration; K_P is the molecular lipid/water partition coefficient, and γ_L being the molar volume of the lipid (0.75 dm^3 mol^{-1}) [25]. All experiments were performed at 25 ± 2°C.

2.5 *Encapsulation of quercetin by multilamellar vesicles (MLVs + QUE)*

Multilamellar vesicles consisting of a mixture of lipids (phosphatidylcholine, phosphatidylglycerol and cholesterol) in different proportions were prepared by the lipid film hydration method using chloroform. Then, quercetin diluted in methanol was added into the lipid mixture at (3:100) quercetin/lipid ratio (w/w). The final mixture was vortexed, and the solvents were evaporated in an atmosphere with N_2, thus obtaining a thin film of dry lipid and quercetin in the flask. After evaporation, the test tube was kept under vacuum for 3 h to completely remove all traces of the organic solvent. The film was hydrated with 20 mmol l^{-1} HEPES buffer, 150 mmol l^{-1} NaF and vortexed (2.5 min) to emulsify and obtain MLVs + QUE. Each formulation was prepared at least three times.

2.6 *Size and zeta potential*

The dynamic light scattering technique was used to evaluate the size and the polydispersity index (PDI) of the formulations. The samples were diluted in 20 mmol l^{-1} HEPES buffer, 150 mmol l^{-1} NaF and analysed in ZetaSizer Nano ZS90 (Malvern Instruments Ltd, Worcestershire, UK). After, the suspension was transferred to a DTS 1060 (Malvern) disposable cuvette with gold electrodes to perform zeta potential measurements through laser Doppler velocimetry experiments, in which the electrophoretic mobility was measured from three measurements. All experiments were performed at least three times and at 25 ± 2°C.

2.7 *Determination of quercetin encapsulation efficiency in MLVs*

Quercetin's entrapment efficiency (%EE) was determined by using UV–Vis's spectrophotometry through a calibration curve of quercetin in methanol, previously constructed and validated at λ = 372 nm. For this, the indirect method of determination was adopted, where 0.5 ml of MLVs + QUE was centrifuged for 10 min at 12000 rpm. The 100 µl of the supernatant was diluted in 1900 µl of methanol and then the concentration was determined by a UV–Vis using the Shimadzu UV 2600 model spectrophotometer (Shimadzu Corp., Japan). After that, equation (2) was used to determine the %EE. All experiments were performed in triplicate in order to ensure good reproducibility of results.

$$\%EE = 100 - \left[\left(\frac{[QUE]supernatant}{[QUE]total}\right) \times 100\right] \quad (2)$$

where $[QUE]_{supernatant}$ is the concentration of quercetin in the supernatant and $[QUE]_{total}$ is the total concentration of quercetin used in the MLVs preparation.

2.8 *In vitro controlled release profile assay*

In vitro release studies of MLVs containing encapsulated QUE were performed in a dialysis bag (cellulose acetate membranes; 18.2 MΩ cm; cut-off = 12.400 MW, Sartorius, Germany), previously prepared with successive washes in deionized water at 60°C. For this, 1350 µl of MLVs + QUE was added to the dialysis membrane and both sides were sealed to avoid leakage. The bags were placed immersed in 30 ml of HEPES buffer pH 7.4 (20 mmol l^{-1} HEPES + 150 mmol l^{-1} NaF) and kept under agitation protected from light. Quercetin release was analysed by extracting 2 ml aliquots of the receptor solution at intervals of 30 min, 1, 2, 3, 4, 5, 6, 24, 48 and 72 h at room temperature. At each withdrawal of 2 ml of an aliquot for analysis, 2 ml of HEPES buffer was added to the medium to keep the volume constant during the experiment. The amount of quercetin released at each time was determined by UV–vis using a Shimadzu UV 2600 spectrophotometer (Shimadzu Corp., Japan). The absorbance obtained in each aliquot was converted into percentage of release using the calibration curve. All experiments were performed in triplicate in order to ensure good reproducibility of results.

2.9 *Application of quercetin release data on mathematical models*

In the present work, the zero-order, first-order, Higuchi as well as Korsmeyer–Peppas (KP) models were used to fitting the experimental data. However, it is important to mention that information about the controlled release mechanisms can only be obtained by the KP model.

Zero-order model: In this model, the release assays from the dosage form may be represented by equation (3) [26]:

$$C_t = C_0 + K_0 \times t, \quad (3)$$

where C_t represents the amount of drug released at time t; C_0 is the initial concentration of drug at time $t = 0$; K_0 is the zero-order rate constant. Thus, zero-order kinetics is associated with a process of constant drug release from a drug delivery system.

First-order model: In the present model, the rate is directly proportional to the concentration of the drug undergoing

reaction, i.e., the greater the concentration, faster the reaction. Hence, it follows linear kinetics (see equation (4)) [26].

$$\log C = \log C_0 - \frac{k_1}{2.303} \times t, \tag{4}$$

where C_0 is the amount of the drug in the formulation before dissolution and k_1 is the first-order release rate constant.

Higuchi model: The release of a bioactive molecule from a drug delivery system involves both dissolution and diffusion. The Higuchi equation is a kinetic relationship widely used in the study of the dissolution of bioactive compounds, which has become an important element in the development of drug release. The Higuchi equation's may be represented by equation (5):

$$Q = K_H \times t^{1/2}, \tag{5}$$

where K_H is the Higuchi dissolution constant; Q is the cumulative amount of bioactive compound released in the time, t.

Korsmeyer–Peppas model (KP): In the model described by KP, the active ingredient release mechanism is a function of the diffusion exponent, n. For a spherical geometry distribution system, $n = 0.43$ suggests a Fickiana diffusion behaviour; for $0.43 < n \leq 0.85$ it corresponds to an anomalous non-Fickian transport (diffusional and relaxational transport) and $n = 0.85$, the release mechanism is related to the relaxational transport [27]. The semi-empirical KP model may be written by equation (6):

$$\frac{M_t}{M_\infty} = K_{kp} \times t^n, \tag{6}$$

where M_t is the active compound release at time t, M_∞ is the amount of compound release for infinite time, K is a constant that considers structural and geometric aspects of the system, and the value of the exponent (n) indicates the release mechanism. The number of atoms that cross a unit area plane per unit of time, determining a particle flux, can evaluate the diffusion process. However, the correlation between the exponent (n) and the diffusive release mechanism is only valid for 60% of the complete release of the active compound. In addition, considering all geometries, anomalous transport represents an intermediate period that corresponds to the application of the diffusive mechanism with zero-order kinetics.

2.10 *Statistical Analysis*

The results obtained were presented as mean ± standard error (SE). Statistics were performed in the Origin Software (version 8.5) using one-way ANOVA analysis followed by Tukey's test. Values of $p<0.05$ were considered significant.

3. Results and discussion

The quercetin's calibration curves were performed in order to quantify the polyphenol throughout the study and guarantee the conditions that best characterize the system of interest. Methanol solution was titrated by quercetin reaching final concentrations from 0 to 50 μmol l^{-1}. The absorbance spectra were recorded and used to obtain the curve shown in figure 1. The results exhibit a linear behaviour respecting the limits of Beer-Lambert law, which is also in good agreement with the data available in the literature [28]. The linear fitting demonstrated a good correlation coefficient, $R^2 = 0.9901$.

To explore the effects of charge and rigidity on the encapsulation of quercetin by MLVs, the lipid mixtures involved the presence of POPC (1-palmitoyl-2-oleoyl-*sn*-glycero-3-phosphocholine) having a zwitterionic polar head (at pH 7.4) and/or POPG (1-palmitoyl-2-oleoyl-*sn*-glycero-3-phosphatidylglycerol) having an anionic one (at pH 7.4) and/or Chol (cholesterol) in distinct proportions (POPC (100%), POPC/POPG (80:20), POPC/Chol (80:20) and POPC/Chol/POPG (60:20:20)) obtained with the same experimental conditions. Then, POPG is the responsible to add the charge properties to lipid compositions, while Chol is able to increase membrane rigidity while maintaining its fluidity [29]. Along this section, most of the results relative to POPC/POPG and POPC/Chol compositions will be compared with those for pure POPC. This strategy will enable to isolate the effects of charge and rigidity in the formulation's average size, size distribution, charge properties besides the encapsulation and release efficiencies of this polyphenol. Similarly, POPC/Chol/POPG results will be compared to the POPC/POPG and POPC/Chol to explore

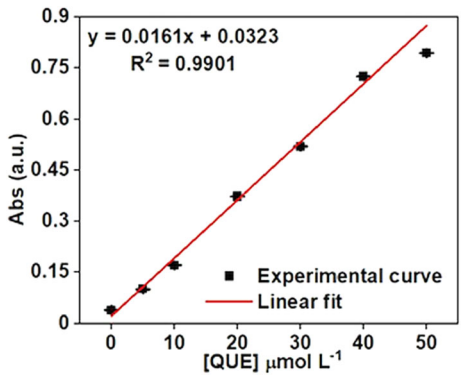

Figure 1. Calibration curve obtained for the quercetin standard using methanol as solvent, λ_{max}=378 nm, at 25 ± 2°C (dots represent the mean of a triplicate and the continuous line is obtained from linear fit).

the effects of the coexistence of charge and rigidity at the same proportions in these parameters.

Spectrophotometric titrations of quercetin (21.5 μmol l^{-1}) by lipid solutions at increasing concentrations (0–600 μmol l^{-1}) were performed to determine the quercetin's partition coefficient (K_P) for the lipid mixtures of interest. This parameter makes it possible to quantify the affinity of the bioactive compound for lipid compositions and can be obtained through the changes observed in the quercetin spectrum due to the addition of lipids, as shown in figure 2a and supplementary figure S1a. The method of second derivatives of the set of spectra was applied, as shown in figure 2b and supplementary figure S1b, to determine the wavelength of maximum absorbance. In the absence of lipid solution, quercetin spectra exhibit a maximum absorbance at 375 ± 3 nm. After lipid addition, polyphenol's absorbance intensity increases, and the maximum wavelength presents a red shift. These observations are indicative that quercetin interacts with lipid systems, moving from an aqueous environment to a more hydrophobic one [30]. The normalized absorbances as a function of lipid concentrations were plotted and adjusted to obtain the partition coefficients, as shown in figure 2c and supplementary figure S1c.

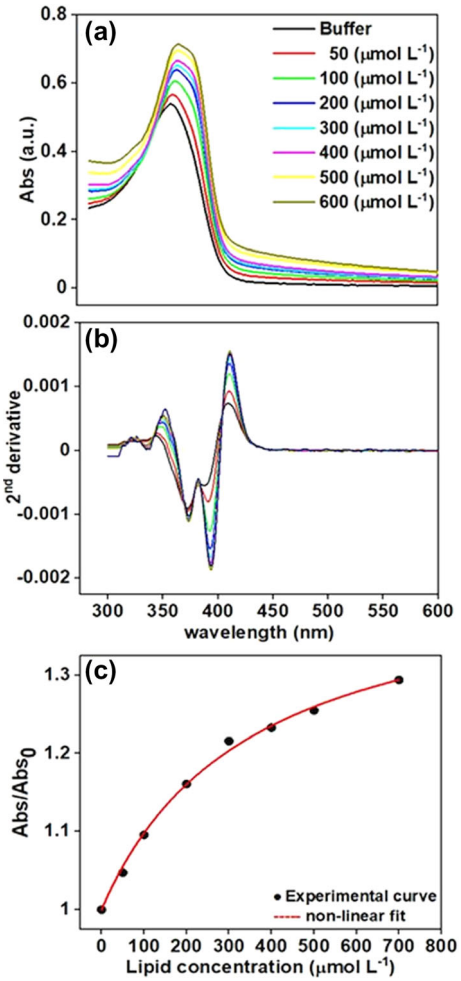

Figure 2. Spectrophotometric titrations of quercetin (21.5 μmol l^{-1}) under increasing lipid concentrations (0–600 μmol l^{-1}). (**a**) Representative quercetin spectral changes as a function of lipid solution addition for POPC/Chol/POPG (60:20:20). (**b**) Second derivatives of the set of spectra shown in (**a**) to determine the wavelength of maximum absorbance. (**c**) Determination of KP values in the presence of POPC/Chol/POPG (60:20:20) LUVs, pH 7.4. Continuous line was obtained using the non-linear fit shown in equation (1). The experiments were performed at 25 ± 2°C.

Table 1 combines the K_P values obtained in this work for the compositions POPC/POPG (80:20) and POPC/Chol/POPG (60:20:20) with the results available in the literature for POPC (100%) and POPC/Chol (80:20) [31]. These data show that quercetin significantly partitions to the lipid systems ($K_P \sim 10^4$). Nonetheless, the presence of anionic lipids reduces the polyphenol affinity by the liposomes. This is probably related to the negative net charge exhibited by quercetin at pH 7.4 [32], which gives rise to electrostatic repulsion between quercetin and lipids. Furthermore, our results for POPC/Chol/POPG confirm the high affinity of quercetin for compositions containing 20% Chol, despite the membrane reduced flaccidity [31]. Once the obtained partitioning coefficient is close to the value found for the POPC composition (100%) [31], the affinity of quercetin for Chol reduces the possible effects of electrostatic repulsion related to the presence of POPG.

The MLVs in the absence and the presence of quercetin encapsulated (MLVs + QUE) were prepared and characterized by dynamic light scattering at each lipid composition. This analysis made it possible to access the average diameter of the obtained structures as well as the degree of homogeneity associated with them through the polydispersity index (PDI) [33,34]. The results are summarized in table 2 and exemplified in supplementary figure S2. The average diameters for POPC (100%), POPC/Chol (80:20) and POPC/Chol/POPG MLVs are greater than 1 μm, which is in good agreement with the literature [35–40]. The MLVs composed of POPC/POPG showed an average diameter of 865 nm representing a reduction of 33% in relation to the result obtained for pure POPC. Negatively charged liposomes have already been shown to present reduced sizes in the literature and this effect may be attributed to the differences in the molecular organization of the lipids [37]. Opposite to this, the presence of cholesterol in the POPC/Chol mixture promoted an increase of 18% in the same

Table 1. Partition coefficient values for each lipid composition.

Lipid composition	K_P (10^4)
POPC (100%)	1.00 ± 0.10[a]
POPC/POPG (80:20)	0.43 ± 0.03
POPC/Chol (80:20)	1.60 ± 0.03[a]
POPC/Chol/POPG (60:20:20)	0.97 ± 0.10

[a]These values were obtained from the study by Leite *et al* [31].

Table 2. Average diameter and PDI values of the different lipid compositions in the absence and in the presence of encapsulated quercetin (mean and SD, $n = 9$, values of $p < 0.05$ were considered significant).

	MLVs		MLVs + QUE	
Lipid composition	Average diameter (nm)	PDI	Average diameter (nm)	PDI
POPC (100%)	1285 ± 126	0.937 ± 0.091	2068 ± 150	0.399 ± 0.053
POPC/POPG (80:20)	865 ± 60	0.114 ± 0.123	605 ± 78	0.350 ± 0.032
POPC/Chol (80:20)	1559 ± 49	1.000 ± 0.008	1884 ± 74	0.350 ± 0.071
POPC/Chol/POPG (60:20:20)	1060 ± 78	0.313 ± 0.252	63 ± 8	0.527 ± 0.042

parameter when compared to the data obtained for PC (100%). In this sense, our findings point out that charge is contributing to the reduction of the average size of the MLVs, while the rigidity is contributing to increase it. In agreement with this observation is the result obtained for the POPC/Chol/POPG mixture. It exhibited an average diameter 18% smaller than that presented for pure POPC, even in the presence of Chol 20% and POPG 20%. The coexistence of charge and rigidity resulted in a system, which the effects observed when POPG and Chol were isolated in the presence of POPC were modulated.

The presence of quercetin promoted changes in the above parameters by influencing the effects attributed to the lipid mixtures. There was a significant increase in the average diameter of the zwitterionic compositions (POPC (100%) and POPC/Chol (80:20)), which can be related to the polyphenol that is encapsulated in the MLVs. However, POPC/Chol (80:20) formulations exhibited lower value than pure POPC, indicating that rigidity decreases MLVs size in the presence of quercetin. In relation to anionic mixtures, the tendency of size reduction was kept and intensified. Interestingly, POPC/Chol/POPG average diameters decreased by two orders of magnitude in relation to the respective MLVs. In this sense, both charge and rigidity contributed to reducing the MLVs + QUE average diameter. The result obtained for the ternary mixture indicates that the combination of Chol and POPG intensify the effects observed when they were isolated in the presence of POPC. As opposed to what was observed in the absence of quercetin. These results show that both the composition and the interaction of the bioactive with the encapsulating system must be considered in the modulation of the size parameter.

The average values of PDI for three independent samples at each lipid composition are shown in table 2. This parameter is used to assess the homogeneity of the system since it is a representation of the distribution of size populations within a given sample [41]. The numerical values of PDI range from 0.0 (for a perfectly uniform sample with respect to particle size) to 1.0 (for a highly polydisperse sample with multiple particle size populations). Our results show values ranging from 0.114 to 1.00 in the absence of quercetin. The highest values are displayed by the POPC (100%) and POPC/Chol compositions. This result reflects the polydisperse character that MLVs have due to their preparation methodology [40]. Comparing the results of these formulations, it is possible to notice that the polydispersity of the system increased in the presence of cholesterol and decreased in the presence of POPG. Opposite to this the results of the other compositions show that the polydispersity of the system decreased in the presence of POPG. These results suggest that the negative charge may be contributing to homogenizing the size distribution of the MLVs while rigidity is acting oppositely. It is reinforced by the result found for POPC/Chol/PG, where the decreased PDI for POPG samples seems to be impaired by the coexistence with cholesterol. In the presence of quercetin, PDI of zwitterionic mixtures was reduced, while the anionic ones increased when compared with the respective data for MLVs. This result can be associated with the anionic character of quercetin at pH 7.4 [32]. The charge added to originally neutral systems has an effect similar to that of POPG on pure MLVs. However, the additional charge due to quercetin in the anionic systems did not contribute to further increase in the homogeneity of the system. This finding suggests that there must be a limit to which the charge factor is able to modulate the PDI parameter.

Zeta potential measurements were also performed for the characterization of the samples. This parameter is derived through electrokinetic mobility measurements and provides information about the surface charge of the studied systems. Figure 3 shows the average values for each formulation (figure 3a) and the boxplots associated with them (figure 3b and c). Pure POPC MLVs showed positive zeta potential values, which are decreased in the presence of POPG and/or Chol. The increased negative potential of POPC/Chol in relation to POPC (100%) agrees with the fact that the inclusion of sterols can alter the order of the phospholipids and the thickness of the bilayer, enabling the realization of hydrogen bonds between lipids and sterols as well as changes in the total charge [18,42–44]. In addition, slightly negative/positive values of ζ in zwitterionic compositions are related to the reorientation of the lipid head groups, due to the lipid phase state and lipid species in dispersion [18]. Jovanović *et al* [18] found zeta potential values around −8 and −10 mV for MLVs composed of POPC and

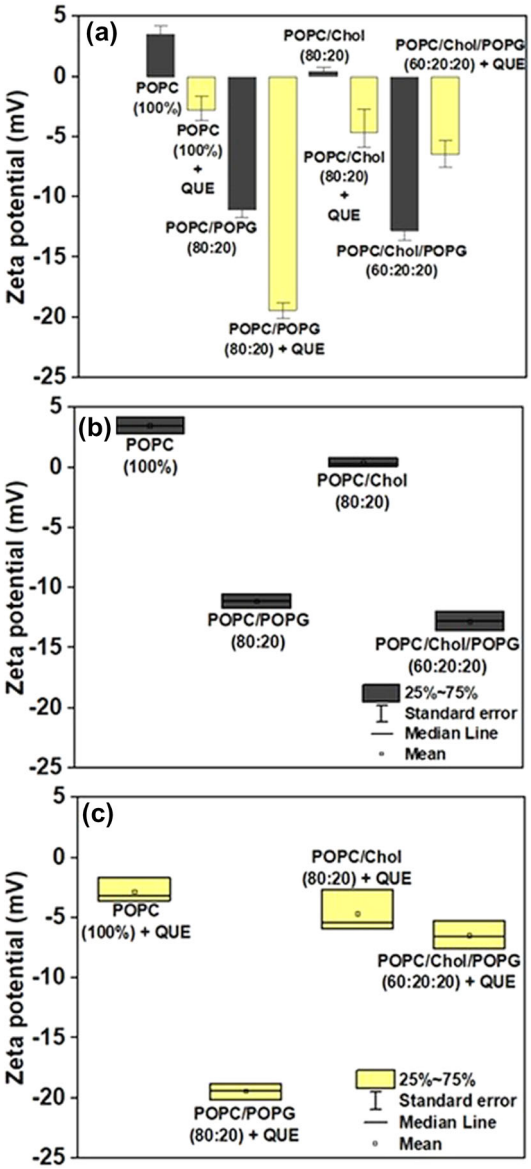

Figure 3. (**a**) Average zeta potential of the tested lipid compositions in the absence and presence of quercetin encapsulated; (**b**) MLVs boxplot with maximum and minimum values, dispersion and symmetry between replicates; (**c**) MLVs + QUE boxplot with maximum and minimum values, dispersion and symmetry between replicates (mean and SE, $n = 9$. Values of $p < 0.05$ were considered significant).

POPC/Chol (80:20), respectively. The differences between these values and our results are related to the electrostatic screening due to the presence of 150 mMol l^{-1} of NaF in our preparations.

MLVs + QUE showed the following average zeta potential values: -2.81 ± 0.5 mV for POPC (100%), -19.43 ± 0.4 mV for POPC/POPG (80:20), -4.66 ± 0.4 mV for POPC/Chol (80:20) and -6.47 ± 0.6 mV for POPC/Chol/POPG (60:20:20). Except for the ternary mixture, the presence of quercetin contributed to the reduction of zeta potential values. The observed decreases in zeta potential due to the presence of quercetin in the following order: $\Delta\zeta = 4.58$mV for POPC/Chol $< \Delta\zeta = 6.31$mV for POPC $< \Delta\zeta = 8.33$ mV for POPC/POPG. These findings are associated with the charge properties of quercetin, as the more it is adsorbed on the surface of MLVs, the more negative the zeta potential can be. The literature shows that quercetin also contributes to increasing the charge properties of similar systems [37,44]. This effect was also observed by Bonechi *et al* [40], which showed that the incorporation of quercetin reduces the zeta potential of zwitterionic DOPC/DOPE (50:50) and anionic DOPE/DOPA (50:50) liposomes by $\Delta\zeta = 2$ and 5 mV, respectively, at 1:1 molar ratio between total lipids and antioxidant. The highest negative zeta potential value was found for POPC/POPG (80:20) (-19.43 ± 0.4 mV). It is related to the anionic character of POPG and quercetin molecules and provides greater stability to the system as nanocarriers. The inclusion of charged molecules in the preparation of MLVs produces electrostatic repulsion between the vesicles, reducing their aggregation and fusion [34,45–49]. In relation to POPC/Chol/POPG, it was expected higher zeta potential values given the presence of POPG. However, it is important to note that MLVs are made up of a set of concentric lipid bilayers. Given the methodology of preparation of MLVs + QUE and the hydrophobic character of quercetin, it is reasonable that the polyphenol is distributed between the internal environment and the surface of the MLVs. The zeta potential allows quantifying only the potential associated with the outer monolayer of these structures and therefore variations such as these can occur. The ternary mixture showed the lowest average diameter and the least homogeneous size distribution in the presence of quercetin, indicating that a synergistic effect between quercetin, cholesterol and POPG resulted in a structure whose molecular organization differs from the other formulations. Figure 3b and c shows the boxplots associated with the dataset obtained for each formulation. This analysis originates from Tukey [50] and shows how the results of each independent measure are distributed around the median and mean of the data. Our results show a symmetrical distribution for most formulations, since the median and mean appear in the centre (or close to the centre) of the boxes. This is an indication that these results constitute a set that represents the system in a satisfactory way from a statistical point of view.

The amount of quercetin encapsulated as a function of MLVs composition was quantified by efficiency tests and the results are shown in figure 4. Encapsulation efficiencies followed the order: POPC/Chol (80:20) > POPC/POPG (80:20) > POPC/Chol/POPG (60:20:20) > POPC (100%), suggesting that the incorporation of Chol and/or POPG in the formulations improved the encapsulation of quercetin in relation to pure POPC. High %EE for quercetin in mixtures containing POPC and cholesterol has already been obtained by Ramli *et al* [51], where 90.1 ± 0.6% was found. Although the highest encapsulation efficiency is found for

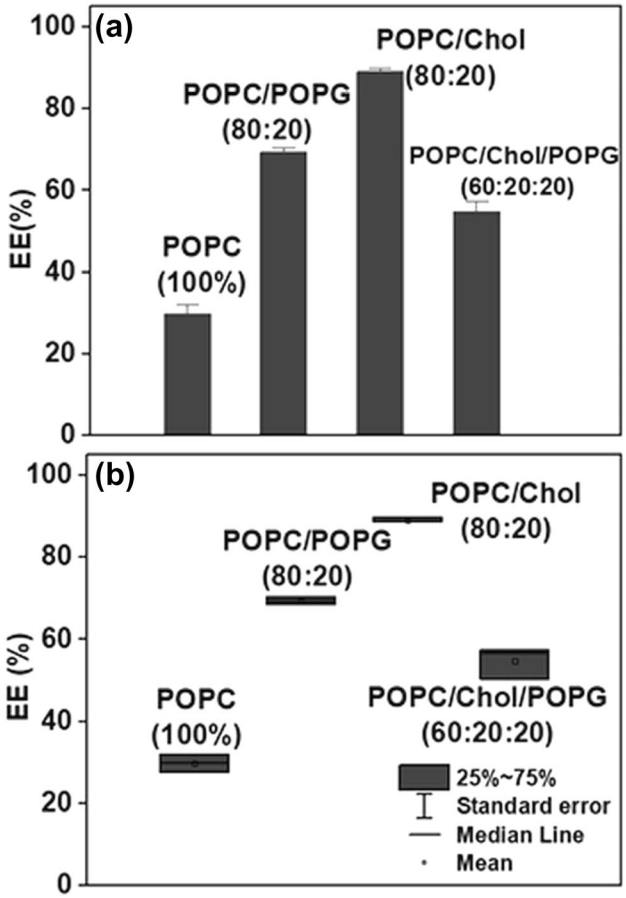

Figure 4. (**a**) Average encapsulation efficiency (%EE) of the tested lipid compositions containing quercetin encapsulated. (**b**) Boxplot with maximum and minimum tails, dispersion and symmetry between replicates (mean and SE, $n = 9$, $p < 0.05$ compared to baseline).

the composition for which quercetin has the greatest affinity, this parameter does not show to be a determinant for quercetin encapsulation. The lipid composition for which quercetin has the lowest affinity has the second-highest encapsulation efficiency. This result suggests that the electrostatic repulsion that may act to reduce the lipid-quercetin affinity does not prevent encapsulation likely driven by non-electrostatic interactions, such as hydrophobic ones. This is reinforced by considering the poorly water-soluble character of quercetin [28,52–55]. Similarly, negatively charged phospholipids have already been shown to be efficient for the encapsulation of curcumin in liposomes, reaching encapsulation efficiencies above 80% and enabling optimal results for slow release and skin deposition [56]. The results for POPC/Chol/POPG (60:20:20) show that the mixture of POPG and Chol reduced the efficiency of encapsulation of the flavonoid, in relation to POPC/POPG and POPC/Chol in accordance with the fact that this composition exhibited the smallest average diameters as displayed in table 2.

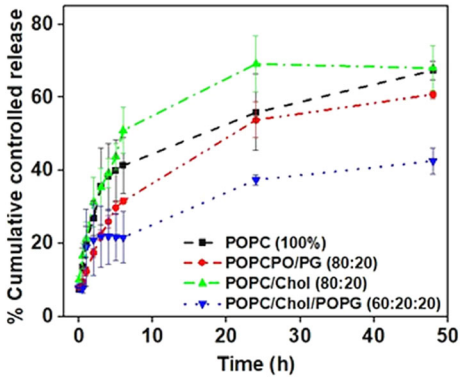

Figure 5. Controlled release assays were obtained at λ_{max} of 378 nm for the quercetin in the different lipid compositions tested.

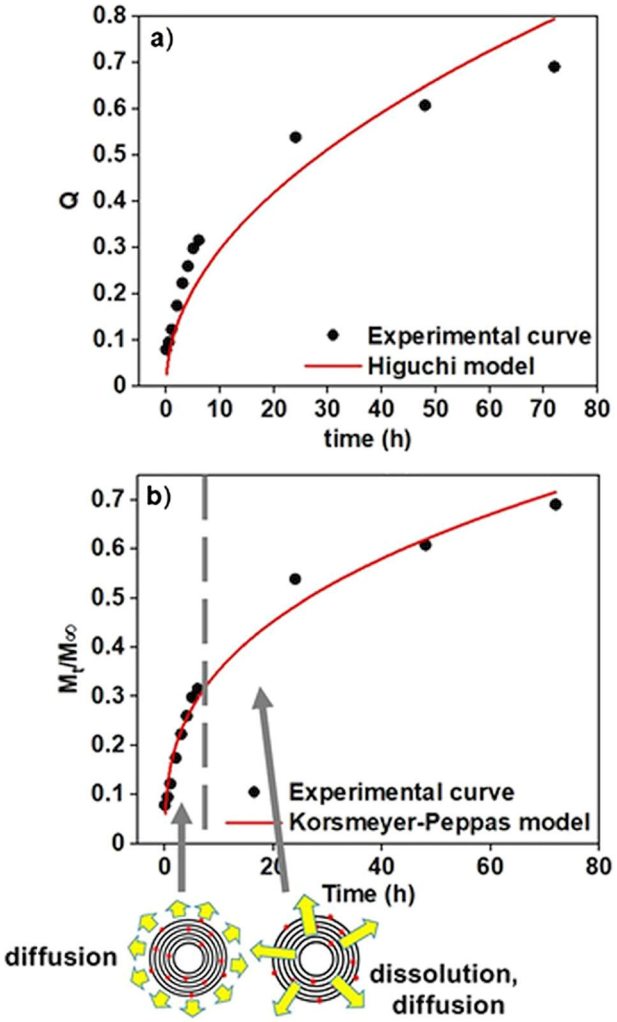

Figure 6. (**a**) Higuchi and (**b**) KP models applied to quercetins kinetic release by POPC/POPG (80:20) formulations, a schematic representation based on Dourado Junior and group [60].

Figure 5 displays the controlled release assays for quercetin encapsulated in the MLVs for each lipid composition. The *in vitro* release profile was obtained by graphing the

Table 3. Parameters obtained through linear fittings for each mathematical model.

	Korsmeyer–Peppas			Higuchi		Zero-order			First-order		
Lipid composition	R^2	n	K_{kp}	R^2	K_H	R^2	K_0	C_0	R^2	K_1	C_0
POPC (100%)	0.93	0.30	0.25	0.47	0.12	0.65	0.66	27.3	0.41	0.01	1.38
POPC/POPG (80:20)	0.98	0.41	0.16	0.88	0.09	0.84	0.82	18.7	0.54	0.01	1.21
POPC/Chol (80:20)	0.89	0.28	0.28	0.37	0.13	0.53	0.62	31.3	0.39	0.01	1.44
POPC/Chol/POPG (60:20:20)	0.95	0.30	0.15	0.46	0.07	0.79	0.47	17.3	0.62	0.01	1.23

R^2 represents the correlation coefficient of each mathematical model; n is the diffusional exponent; K_{kp} is the Korsmeyer release rate constant (μg h^{-1}); K_H is the Higuchi's dissolution constant or Higuchi's release constant; K_0 is the zero-order rate constant; C_0 is the initial concentration of drug at time $t = 0$; K_1 is the first-order rate equation expressed in time (per hour).

cumulative percentage of the polyphenol release with respect to the amount encapsulated as a function of time (M_t/M_∞ *vs. t*). All formulations exhibited significant release that is dependent on the lipid composition. The lowest rate of release was obtained for POPC/Chol/POPG (60:20:20), consistent with our results for this same composition that show structures of reduced average size and moderate encapsulating ability of quercetin. Furthermore, the stiffening effect of the lipid bilayer by cholesterol must be considered and may be interfering with this process. Evidence of this effect is also seen in the release of quercetin by POPC/Chol (80:20) composition, where the highest content of encapsulated quercetin is followed by an attenuated release. Being equivalent to the one observed in the formulation that shows the lowest encapsulation efficiency, POPC (100%). Besides, this result corroborates the fact that the flavonoid has the greatest affinity for POPC/Chol composition, which could also impair the release kinetics. In line with this, POPC/POPG is the composition for which the lowest partition coefficient was presented and exhibits the highest release rate.

The initial faster rate of release observed for all formulations is commonly ascribed to bioactive detachment from the outer surface, while the later slow release is due to sustaining quercetin release from the inner core of the MLVs [57]. Kinetic evaluation of quercetin release profiles in the distinct lipid compositions was also performed, to elucidate the mechanisms involved in the bioactive release from the studied systems. The zero-order, first-order and Higuchi models were used to fitting our results, while the Korsmeyer–Peppas (KP) mathematical model was used to understand the mechanisms of controlled release. Figure 6 exhibits only the best fittings obtained in the present work. Table 3 displays the obtained parameters for each model. As can be seen the most appropriate adjustments for our systems were obtained using the Higuchi and Korsmeyer–Peppas models. It is important to mention, the Korsmeyer–Peppas model was the one that showed the best correlation coefficient, R^2 for the 60% release, demonstrating the mentioned model was able to describe the drug release kinetics from liposomes [57–60]. The release of quercetin for our formulations follows Fick's law ($n \leq 0.43$, see table 3) [57,58]. As well described in the literature [61–65], when the diffusion exponent assumes values of $n < 0.43$ are indicative of release mechanisms that follow Fick's law. Intermediate values $0.43 \leq n \leq 0.85$ suggest anomalous behaviour with a non-Fickian release, while $n > 0.85$ indicates that the mechanism is governed by relaxation processes of the polymeric matrix, defined as case II type transport. Finally, our results demonstrated that despite the differences triggered by the lipid compositions pointed out throughout this study, the release assays were not susceptible to these changes.

4. Conclusions

In this work, we describe our findings on the effect of different lipid compositions on the encapsulation of quercetin by MLVs. Our results showed that the affinity of quercetin for lipid systems is dependent on the lipid composition, with partition coefficients in the order of 10^4. The MLVs + QUE formulations were characterized by dynamic light scattering and zeta potential measurements, while the encapsulation and release efficiencies were performed via spectrophotometry. This strategy showed that the rigidity, imposed by Chol, increased both the homogeneity of the size distribution and the encapsulation efficiency of the POPC/Chol system, enabling a significant rate of quercetin release. The presence of charge due to POPG resulted in remarkable effects, as it modulated both the average size and size distribution of the POPC/POPG formulation, as well as resulted in high encapsulation and release efficiencies. However, the combination of rigidity and charge in the POPC/Chol/POPG formulation gave rise to the smallest average diameter, greatest heterogeneity in size distribution and the lowest release efficiency. The release kinetics of quercetin were analysed using Higuchi and Korsmeyer–Peppas models and showed that the mechanism by which quercetin release is independent of the lipid composition

following Fick's law. In this sense, this work sheds light on the effect of lipid composition at important parameters in the development of nano and microcarriers where additional efforts are welcome, especially in understanding the mechanisms involved in this.

Acknowledgements

NBL slade acknowledges the financial support from Research Supporting Foundation of Minas Gerais State (FAPEMIG-Brazil; Grant APQ-00554-21). J A Moreto would like to acknowledge the financial support received from the National Council of Technological and Scientific Development (CNPq-Brazil; Grant 303659/2019-0) and Research Supporting Foundation of Minas Gerais State (FAPEMIG-Brazil; Grant APQ-02276-18). We are thankful to Prof. Dr M P dos Santos Cabrera for donating the quercetin sample, Prof. Dr J Ruggiero Neto for the use of the ZetaSizer Nano ZS90 (Malvern Instruments Ltd, Worcestershire, UK), Prof. Dr P I S Maia and the Biochemistry Department of UFTM for the structures and equipment made available. Mendes also thanks the Coordination for the Improvement of Higher Education Personnel (CAPES) for the scholarship and Graduate Program in Materials Science and Technology (PPGCTM-UFTM).

References

[1] Gorbenko N I, Borikov O Y, Kiprych T V, Ivanova O V, Taran K V and Litvinova T S 2021 *Endocr. Regul.* **55** 182
[2] Zhou J, Fang L, Liao J, Li L, Yao W, Xiong Z *et al* 2017 *PLoS One* **12** e0172838
[3] Zhao L, Cen F, Tian F, Li M, Zhang Q, Shen H *et al* 2017 *Exp. Ther. Med.* **14** 5942
[4] Kalbassi M R, Behzadi T M and Paknejad H 2021 *Iran Fish. Sci. J.* **30** 39
[5] Oguz M, Dogan B, Durdagi S, Bhatti A A, Karakurt S and Yilmaz M 2021 *New J. Chem.* **45** 18443
[6] Khursheed R, Singh S K, Wadhwa S, Gulati M, Kapoor B, Jain S K *et al* 2021 *Int. J. Biol. Macromol.* **189** 744
[7] Morante-Zarcero S, Endrino A, Casado N, Pérez-Quintanilla D and Sierra I 2021 *J. Porous Mater.* **28** 1
[8] Shaji J and Iyer S 2012 *Asian J. Pharm.* **6** 218
[9] Berbel M E, Paiva A M, Chiari-Andréo B G, Lallo S B, Oshiro-Júnior J Á and Chiavacci L 2017 *Int. J. Nanomed.* **12** 4991
[10] Bandara S, Molley T G, Kim H, Bharath P A, Kilian K and Leal C 2019 *Mater. Horizons* **7** 125
[11] Schwendener R A 2014 *Ther. Adv. Vaccines* **2** 159
[12] Jash A, Ubeyitogullari A and Rizvi S S H 2021 *J. Mat. Chem. B* **9** 4773
[13] Omolo C A, Hassan D, Devnarain N, Jaglal Y, Mocktar C, Kalhapure R S *et al* 2021 *Colloids Surf. B* **207** 112043
[14] Huh S Y, Shin J W, NA J I, Huh C H, Youn S W and Park K C 2010 *J. Dermatol.* **37** 311
[15] Apolinário A C, Pachioni-Vasconcelos J A, Pessoa A Jr and Rangel Yagui C O 2017 *Quim. Nova* **40** 810
[16] Van Meer G, Voelker D R and Feigenson G W 2008 *Nat. Rev. Mol. Cell Biol.* **9** 112
[17] Epand R M 1998 *Biochim. Biophys. Acta* **1376** 353
[18] Jovanović A A, Balanč B D, Ota A, Grabnar P A, Djordjević V B, Šavikin K P *et al* 2018 *Eur. J. Lipid Sci. Technol.* **120** 1800039
[19] Henriksen J, Rowat A C and Ipsen J H 2004 *Eur. Biophys. J.* **8** 732
[20] Arriaga L R, Lopez-Montero I, Monroy F, Orts-Gil G, Farago B and Hellweg T 2009 *Biophys. J.* **96** 3619
[21] Alvares D S, Monti M R, Ruggiero Neto J and Wilke N 2021 *Biochim. Biophys. Acta Adv.* **1** 100002
[22] Goñi F M, Alonso A, Bagatolli L A, Brown R E, Marsh D, Prieto M *et al* 2008 *Biochim. Biophys. Acta-Mol. Cell Biol. Lipids* **1781** 665
[23] De Almeida R F M, Fedorov A and Prieto M 2003 *Biophys. J.* **85** 2406
[24] Santos N C, Prieto M and Castanho M A R B 2003 *Biochim. Biophys. Acta-Biomembr.* **1612** 123
[25] Marsh D 2010 *Chem. Phys. Lipids* **163** 667
[26] Baishya H 2017 *J. Dev. Drugs* **6** 1000171
[27] Silva R T C, Dalmolin L F, Moreto J A, Oliveira C G, Machado A E H, Lopez R F V *et al* 2020 *J. Nanopart. Res.* **22** 239
[28] Suman S, Roy A, Bahadur S and Choudhury A 2018 *Res. J. Pharm. Technol.* **11** 61
[29] Kahya N and Schwille P 2006 *J. Fluoresc.* **16** 671
[30] Rich G T, Buchweitz M, Winterbone M S, Kroon P A and Wilde P J 2017 *Nutrients* **9** 111
[31] Leite N B, Martins D B, Alvares D S and Cabrera M P S 2022 *Chem. Phys. Lipids* **20** 242
[32] Sanver D, Sadeghpour A, Rappolt M, Di Meo F and Trouillas P 2020 *Langmuir* **40** 11776
[33] Jindal S, Awasthi R, Singare D and Kulkarni G T 2021 *J. Res. Pharm.* **25** 34
[34] Pivetta T P, Silva L B, Kawakami C M, Araujo M M, Del Lama M P F M, Naal R M Z G *et al* 2019 *J. Drug Deliv. Sci. Technol.* **53** 101148
[35] Pinheiro M, Lúcio M, Lima J L and Reis S 2011 *Nanomed.* **6** 1413
[36] Fatouros D G and Antimisiaris S G 2002 *J. Colloid Interface Sci.* **251** 271
[37] Lawrence S, Alpar H, McAllister S and Brown M 1993 *J. Drug Target.* **1** 303
[38] Espiritu R A, Cornelio K, Kinoshita M, Matsumori N, Murata M, Nishimura S *et al* 2016 *Biochim. Biophys. Acta* **1858** 1373
[39] Bangham A D 1968 *Prog. Biophys. Mol. Biol.* **18** 29
[40] Bonechi C, Donatia A, Tamasi G, Leone G, Consumi M, Rossi C *et al* 2018 *Biophys. Chem.* **233** 55
[41] Danaei M, Dehghankhold M, Ataei S, Hasanzadeh Davarani F, Javanmard R, Dokhani A *et al* 2018 *Pharmaceutics* **10** 57
[42] Ricci M, Olivia R, Del Vecchio P, Paolantoni M, Moressi A and Sassi P 2016 *Biochim. Biophys. Acta* **1858** 3024
[43] Bhattacharya S and Haldar S 2000 *Biochim. Biophys. Acta* **1467** 39

[44] Mandić L, Sadžak A, Strasser V, Baranović G, Domazet Jurašin D, Dutour Sikirić M *et al* 2019 *Int. J. Mol. Sci.* **20** 2709
[45] Sciolla F, Truzzolillo D, Chauveau E, Trabalzini S, Di Marzio L, Carafa M *et al* 2021 *Colloids Surf. B* **208** 112054
[46] Mano C M, Guaratini T, Cardozo K H M, Colepicolo P, Bechara E J H and Barros M P 2018 *Drugs* **16** 126
[47] Váňová J, Laura J L, Petr Č and Susanne K W 2017 *Cogent. Chem.* **3** 1385173
[48] Paquet-Côté P A, Tuck K L, Paradis J P, Graham B and Voyer N 2017 *Tetrahedron Lett.* **58** 4672
[49] Batista C M, Carvalho C M B and Magalhães N S S 2007 *Ver. Bras. Cienc. Farm.* **43** 167
[50] Tukey J W (eds) 1977 *Exploratory data analysis* (Massachusetts: Addison-Wesley) p 27
[51] Ramli N, Nora'aini A and Hamzah S 2020 *J. Sustain Sci. Manag.* **15** 15
[52] Toniazzo T, Peres M S, Ramos A P and Pinho S C 2017 *Food Biosci.* **19** 17
[53] Huang M, Su E, Zheng F and Tan C 2017 *Food Funct.* **8** 3198
[54] Codevilla C, Bazana M, Silva C and Barin J M C 2015 *Cienc. Nat.* **37** 142
[55] Geethi P, Veranja K D and Nedra K 2016 *J. Nanomater.* **2016** 1
[56] Kumar R, Choudhary D K and Debnath M 2020 *Mater. Res. Express.* **7** 1
[57] Mura P, Maestrelli F, D'Ambrosio M, Luceri C and Cirri M 2021 *Pharmaceutics* **13** 437
[58] Haghiralsadat F, Amoabediny G, Helder M N, Naderinezhad S, Sheikhha M H, Forouzanfar T *et al* 2018 *Artif. Cells Nanomed. Biotechnol.* **46** 169
[59] Jain A and Jain S K 2016 *Chem. Phys. Lipids* **201** 28
[60] Faria D M, Dourado Júnior S M, Nascimento J P L, Nunes E S, Marques R P, Rossino L S *et al* 2016 *Mater. Res.* **20** 225
[61] Dourado Junior S M, Nunes E S, Marques R P, Rossino L S, Quites F J, Siqueira Junior J R *et al* 2017 *J. Mater. Sci.* **52** 9491
[62] Siepmann J and Siepmann F 2006 *Prog. Colloid Polym. Sci.* **133** 15
[63] Huang X and Brazel C S 2001 *J. Control. Release* **73** 121
[64] Siepmann J, Faisant N and Benoit J P 2002 *Pharm. Res.* **19** 1885
[65] Siepmann J and Peppas N A 2001 *Adv. Drug Deliv. Rev.* **48** 139